Received: 3 September 2017 | Revised: 30 July 2019 | Accepted: 15 August 2019

DOI: 10.1111/twec.12860

ORIGINAL ARTICLE

The World Economy WILEY

A global compass for the great divergence: Emissions versus production centres of gravity 1820–2008

Caspar Sauter[1] | **Jean-Marie Grether**[2] | **Nicole A. Mathys**[3]

[1]UBS SA, Zurich, Switzerland

[2]University of Neuchatel, Neuchatel, Switzerland

[3]Federal Office for Spatial Development, Bern, Switzerland

Funding information

Swiss National Science Foundation, Grant/Award Number: Grant 100018-136625

KEYWORDS

center of gravity, GDP and CO_2 emissions, great divergence

1 | INTRODUCTION

The need for global indicators to address large-scale socioeconomic issues is today more acute than ever. Human societies have become so opulent, ubiquitous and interconnected that many of the challenges they face, from climate change to security, find their roots and/or unravel consequences all around the planet. In spite of this globalisation of economic problems, most measurement tools used by analysts and policymakers remain national in scope (e.g. Lindmark, 2004), or simply aggregated at the world level, without considering the geographical dimension except in specific cases (e.g. indicators of remoteness, Baier & Bergstrand, 2009 or geopolitical importance, Reynaud & Vauday, 2009, but which are country-specific in nature). In this paper, we propose to revisit and refine the concept of the world centre of gravity, which encapsulates into a single point the distribution of any variable upon the earth's surface. We apply it to human population, gross domestic product (GDP) and anthropogenic carbon dioxide (CO_2) emissions, uncovering crucial but not trivial trends across the 1820–2008 period.

Early applications of the centre of gravity (see Grether & Mathys, 2010; Quah, 2011) focused on GDP and recent decades. They unveiled a clear Eastern shift of the economic centre of gravity since 1980. Two subsequent papers (Grether & Mathys, 2011; Grether, Mathys, & Lutzelschwab, 2012) extended the time period backwards, relying on the Maddison (2010) database. They identified a strong Western shift of the economic centre of gravity during the nineteenth century and a trend

reversal towards the east in 1950. Although informative, these early studies are subject to three type of limitations: first, the reported evidence so far is limited in its scope and its contribution to the understanding of world challenges; second, the degree of accuracy depends on the availability and reliability of gridded data on the earth's surface for the relevant variables; third, the centre of gravity itself is a point beneath the earth's surface, which is not entirely intuitive and leads to distortions when its position is projected upon a two-dimensional map. The objective of the present paper is to provide an appropriate treatment of each of these caveats, thereby illustrating the usefulness of the approach.

The inclusion of CO_2 emissions, along with GDP and population, allows for deeper insights into the period of the so-called 'Great Divergence'. Following Zhao, Stough, and Li (2003), we use the demographic centre of gravity as a benchmark and construct simple measures of spatial imbalances to characterise the divergence between world GDP (or emissions) and world population. As could be expected, the two indices follow a similar inverted-u pattern over the centuries of the Great Divergence, but with two important differences: (a) the starting level of spatial imbalances for emissions is considerably larger than for production and (b) the trend reversal occurs 30 years earlier for emissions (1920) than for GDP (1950). This illustrates the historic responsibility of the west, a cornerstone of the present negotiations to tackle climate change (e.g. Barrett & Stavins, 2003 or Mattoo & Subramanian, 2012). It also proves how deeply associated are energy use and transition with the economic divergence or convergence processes (e.g. Bradshaw, 2014). Finally, it suggests that the industrial revolution was already full steam ahead when it began to materialise into significant shifts in economic power. This is in line with recent advances in economic history pointing to early roots of the process, perhaps as far back as the sixteenth century (e.g. Broadberry, 2013 or Studer, 2015).

An important limitation of all previous studies is that, for all years for which gridded data are unavailable, the assumption is simply that grid shares at country level are unchanged with respect to the closest available year (e.g. 1990 for the papers based on the G-Econ database, see Nordhaus et al., 2006). This is of particular concern for countries like the United States or China, which cover large areas, represent a significant share of world totals, and where the distribution of people and economic activity has seen structural changes over the last two centuries. The present paper offers an improvement with respect to that shortcoming, by exploiting the Hyde 3.1 database (Klein Goldewijk, Beusen, Drecht, & Vos, 2011), which provides gridded population data at a very disaggregated level. This goes back as far as 1750 and has already been exploited by long run studies of land use by human populations (Ellis et al., 2013) and its relationship with global warming (Matthews et al., 2014). It allows to spread national totals regarding GDP (or CO_2 emissions) according to varying population shares rather than by applying fixed shares.

Although the centre of gravity ought to be seen as the tip of a global arrow originating from the centre of the earth, its representation on a two-dimensional map is subject to distortions. The methodological section provides a thorough discussion of distortions relying on the two projection methods used so far (i.e. the orthogonal projection on the earth's surface or onto a cylinder wrapping the earth along the Equator). We then propose a new technique, which is distortion-free, and consists of using two maps instead of one to represent the three Cartesian coordinates of the centre of gravity. This allows more precise tracking of the centre of gravity.

In short, the centre of gravity behaves like a global compass, with its length and direction depending on the spatial distribution of the corresponding variable upon the earth's surface. Its calculation and comparisons across key socioeconomic indicators allows unveiling global shifts and spatial unbalances over the sample period. This may justify further applications of the concept in a number of different domains, as suggested in the conclusion.

2 | METHODOLOGY

2.1 | Cartesian coordinates of world centres of gravity

Assume the surface of the earth is covered by a regular grid of N cells. Each cell i, $i = 1,\ldots, N$, is identified by the latitude (ϕ) and longitude (λ) of its lower-left corner. For each cell, there is an estimate of the underlying variable V, that is CO_2 emissions (E) for the world emission centre of gravity, GDP (G) for the world economic centre of gravity or population (P) for the world demographic centre of gravity.

The Cartesian coordinates of each centre of gravity are determined according to the three-step methodology previously introduced by Grether and Mathys (2010). First, the share of each cell in the world total is calculated, that is $s_{iV} = V_i \Big/ \sum_{i=1}^{N} V_i$. Second, the Polar coordinates of each grid cell are converted into their corresponding Cartesian coordinates, denoted by x, y and z. For that purpose, the earth is assumed to be a perfect sphere, a reasonable assumption given the approximations affecting the measurement of the underlying variables. Cartesian coordinates may be expressed in kilometres, or as a fraction of the earth's radius, R (6,371 km).[1] Third, the coordinates of the world centre of gravity are obtained as weighted averages of the Cartesian coordinates of each grid cell, using grid cell shares as weights:

$$x_V = \sum_{i=1}^{N} s_{iV} x_i, y_V = \sum_{i=1}^{N} s_{iV} y_i, z_V = \sum_{i=1}^{N} s_{iV} z_i. \quad (1)$$

The obtained point, $P_V^* = (x_V, y_V, z_V)$, where $V = E, G, P$ locates within the sphere. The length of the associated vector, with its origin in the earth's centre, is obtained as:

$$\left\| \overrightarrow{OP_V^*} \right\| = \sqrt{(x_V)^2 + (y_V)^2 + (z_V)^2}. \quad (2)$$

This length can be used as a rough indicator of the concentration of the underlying variable on the earth's surface. An extreme concentration in a single point would lead to a gravity centre right on the earth's surface and a length just equal to the earth's radius.[2]

2.2 | Existing conventions to represent the location of world centres of gravity

The literature on how to map the earth's surface on a two-dimensional plane dates back more than two thousand years (see Snyder, 1987 for a detailed survey including both technical and historical references). There is no universally accepted technique, as every method (cylindrical, conic or azimuthal, and their subcases) presents its shortcomings regarding specific distortions (e.g. on distances, areas or angles). The problem is further compounded here by the fact that the points we are interested in, that is, centres of gravity, are located within the sphere, not on its surface.

To the best of our knowledge, two projection techniques have been proposed for the world centres of gravity, as illustrated by Figure 1. The first, proposed by Grether and Mathys (2010), consists of projecting orthogonally the centre of gravity, P^*, upon the earth's surface (Figure 1a). It leaves

[1] In a 3-dimensional space where the origin is at the centre of the earth, axis x (projection of the Greenwich meridian) and axis y (projection of the 90°E meridian) define the equatorial plane, and axis z is the north–south polar axis, the corresponding formulas are as follows: $x_i = R\cos(\phi_i)\cos(\lambda_i)$, $y_i = R\cos(\phi_i)\sin(\lambda_i)$, $z_i = R\sin(\phi_i)$, where R is the earth's radius. See the technical Appendix to Grether and Mathys (2011) for a detailed description.

[2] If the spatial distribution of the underlying variable is multimodal, a centre of gravity close to the earth's centre does not necessarily imply less concentration. See Grether and Mathys (2011) for discussion.

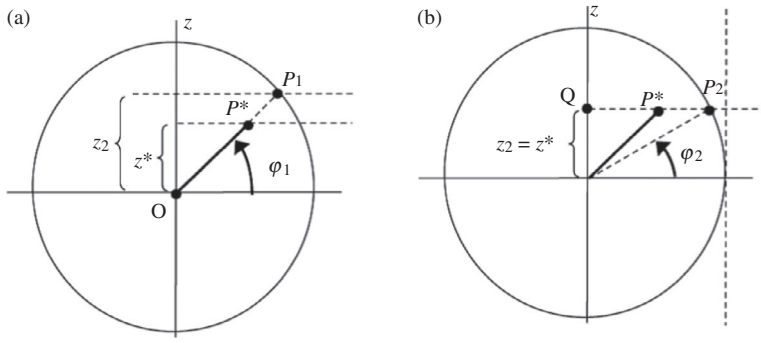

FIGURE 1 Alternative projections of the world's centre of gravity. (a) Grether and Mathys (2010). (b) Quah (2011)

unspecified the technique used to represent the projection point, P_1, with latitude ϕ_1. The second technique, proposed by Quah (2011), directly projects the centre of gravity on a cylinder wrapping the globe along the Equator (Figure 1b), which leads to a lower latitude for the projection point, $\phi_2 < \phi_1$.

Both techniques may be criticised on the grounds that they are insensitive to specific directional movements of the centre of gravity, depending on the distribution of the underlying variable over time: Grether and Mathys (2011) do not capture changes of P^* along the OP_1 axis; Quah (2011) is insensitive to changes of P^* along the QP_2 line. Which type of change matters more in practice is an empirical question, which could guide the choice between these two techniques (or any alternative deemed more relevant depending on the specific variable or time period considered). However, any convention relying on a single two-dimensional map will remain affected by some kind of distortion. That is why we privilege here Cartesian over Geographic coordinates and use two maps instead of one.

2.3 | A new, distortion-free convention

The first map, on the left of Figure 2, is consistent with Quah (2011), that is a cylindrical projection. It provides, on the vertical axis, a distortion-free representation of the z Cartesian coordinate described above. The horizontal axis represents longitude, which is subject to distortions, because there is an infinity of (x, y) combinations within the sphere corresponding to the same longitude. The second diagram provides an explicit representation of x and y, with the $x(y)$ axis representing the projection of the Greenwich (90°) meridian. All three Cartesian coordinates are expressed as a fraction of the earth's radius.[3]

The combination of these two maps permits describing without distortion any underground movement of the centre of gravity, including those peculiar cases to which previously used conventions are insensitive. Two stylised examples will help to illustrate the complementarity of both maps. In each case, one of the two maps gives a confusing vision of the evolution of the centre of gravity, while the other unveils what actually happens. We dub the first case the 'wipper effect'. It is represented in Figure 3, where the left map suggests that the centre of gravity shifts from A to B, then back again and so forth, as a pendulum covering apparently the same horizontal distance period after period. However, what happens in reality, as shown by the right map, is that the centre of gravity gets ever closer to the centre of the earth, along a zigzag trajectory. Again, this illusion is due to the fact that an infinity of within-sphere (x, y) combinations is compatible with the same longitude.

[3]Countries' contours correspond to a Lambert equal-area cylindrical projection in the left map and to an azimuthal projection in the right map. Figures 2–4 limit the number of meridians and parallels to streamline presentation. Consecutive figures with actual results report meridians and parallel every 10°, along with ticks to indicate half of the earth's radius on the –x, y and z axes.

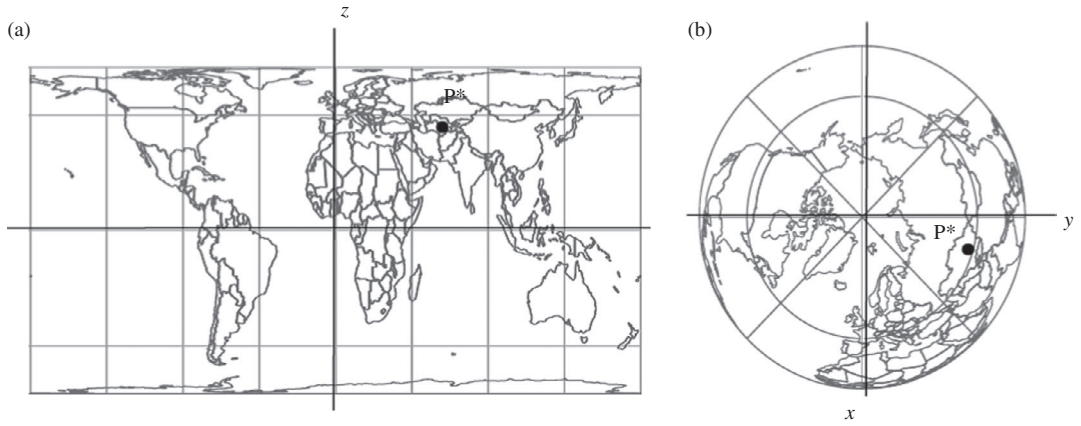

FIGURE 2 Cartesian coordinates of the gravity centre on two maps. (a) Cylindrical projection. (b) Azimuthal projection

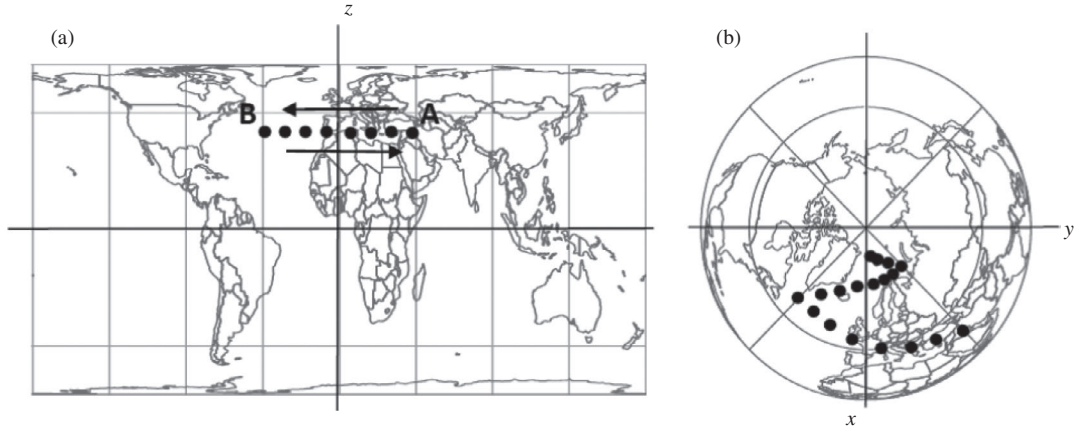

FIGURE 3 The 'wiper' effect

The right map is not exempt from optical illusion either however. In the second case, illustrated in Figure 4, the centre of gravity appears to be going round a regular ellipse on the right map. However, the left map shows that its height above the equatorial plane is regularly decreasing. We call that movement along a downward spiral 'staircase' effect.

Other optical illusions could still be considered but are not reported here for the sake of conciseness, and as we limit the presentation to the two cases which do affect our results. The key point is that, although we keep on using latitudes and longitudes to characterise locations on maps, the centre of gravity is an underground point which is best identified in space by using three Cartesian coordinates rather than two Geographic coordinates.

3 | DATA SOURCES

Data are obtained by combining five distinct sources. Three databases provide information at the grid level. The HYDE 3.1 database (Klein Goldewijk et al., 2011) provides historical gridded population data from 10,000 B.C to 2005 A.D. Since 1820, the data are available in 10-year intervals and have a

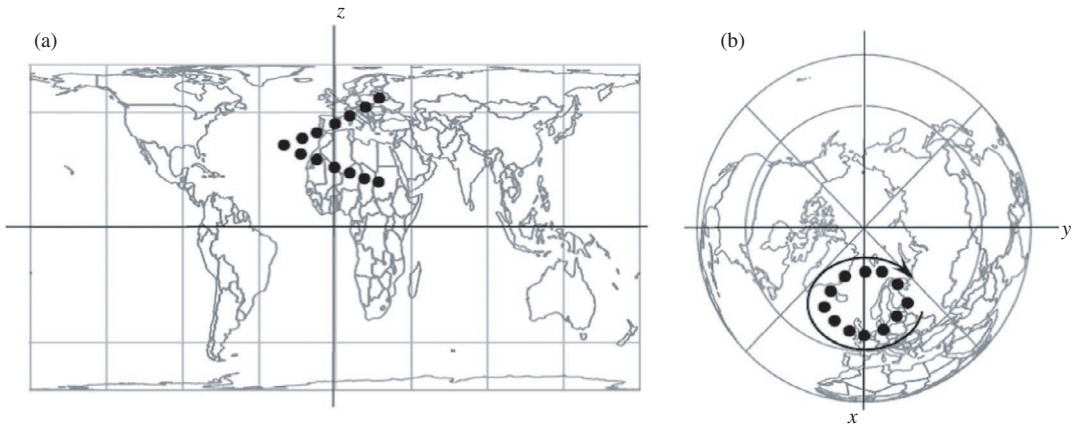

FIGURE 4 The 'staircase' effect

grid resolution of 5-by-5 arc minutes (one arc minute is equal to 1/60 of 1°). The G-Econ research project (see G-Econ, 2011) provides gridded GDP data at a one degree level of resolution for the years 1990, 1995, 2000 and 2005. The Emission Database for Global Atmospheric Research (EDGAR, see European Commission & Joint Research Centre/Netherlands Environmental Assessment Agency, 2011) reports yearly data on CO_2 emissions from fuel combustion and nonmetallic mineral processes (including cement production),[4] excluding short-cycle organic carbon from biomass burning at a 0.1° level of resolution. These data cover the period 1970–2008. Two other databases cover larger periods but at the national level only. The Maddison Project (2013) contains estimates of GDP and population from 1 to 2010 A.D., and the Carbon Dioxide Information Analysis Center (CDIAC, see Boden, Marland, and Andres (2013)) provides CO_2 estimates from fossil fuel consumption and cement production over the 1751–2010 period.

3.1 | Population

The only modification of the HYDE database is to extend it from 2005 to 2010. To do so, we apply to each cell's population in 2005 the population growth rate 2005–10 of the corresponding country as obtained from the Maddison database. Country attribution of each cell is obtained by merging HYDE with the Global Database on Administrative Boundaries (GADM, 2012). As explained below, this HYDE gridded population database at a very high degree of resolution provides the basis to extend GDP and emission gridded data backward in time.

3.2 | Gross domestic product

First, the G-Econ 2005 gridded GDP data are extended to 2010, using Maddison country real GDP data for growth rates and by relying on the same method for population. Second, we extend the gridded GDP series backward to 1820 by combining the HYDE and Maddison databases by assuming that within-country GDP is uniformly distributed per capita. This allows us to spread national GDP figures from the Maddison database according to the gridded population shares obtained from the HYDE

[4]Note that EDGAR covers more carbon dioxide sources, but to correctly match EDGAR with CDIAC (which covers only CO_2 emissions from fossil-fuel consumption and cement production), we retain from EDGAR only CO_2 emissions from IPCC source category 1A (fuel combustion) and 2A (non-metallic mineral processes).

TABLE 1 Summary statistics (world level): Aggregated Population (persons), GDP (1990 US$) and CO_2 (gigagrams), 1820–2010

	1820	2010	Annual growth rate 1820–2010 (%)
Population	1.04E + 09	7.23E + 09	1.03
GDP	7.32E + 11	6.49E + 13	2.42
CO_2	15,760	1.02E + 07	3.60

database. The figures obtained are of course an approximation, but given data availability, it is the best way to capture within-country spatial variations backward in time. We then aggregate these 5 arc minutes cells to cells with a 60 arc minutes resolution to match them with the G-Econ data. Finally, we merge the Maddison/HYDE data, covering the decades 1820–2000, with the G-Econ database, which covers the years 1990–2010.[5] Whenever possible, we construct 5-year averages around decimal years to minimise the influence of potential extreme events.

3.3 | CO_2 emissions

The procedure is similar to that followed for GDP. First, gridded EDGAR emission data for 2008 are extended to 2012 using 2008–10 and 2010–12 national growth rates obtained from the EDGAR FT2012 database. Second, to extend data backward in time, the HYDE and CDIAC databases are combined assuming emissions per capita are uniformly spread within countries. Then, the data are aggregated to a 60 arc minutes resolution to harmonise with the GDP aggregation level. Finally, we merge the CDIAC/HYDE data, covering the years 1820–1990 with the EDGAR database which covers the years 1970 to 2010.[6] Whenever possible, we construct 5-year averages around decimal years to minimise the influence of potential extreme events.

Tables 1 and 2 report summary statistics for each variable. Table 1 reports summary statistics for yearly series (1820 and 2010) that have been aggregated over all cells; Table 2 reports summary statistics at the cell level for 1820 and 2010.

4 | RESULTS

Figures 5–7 report the two-map diagrams for the three centres of gravity. We remind the reader that the country frontiers are only reported for graphical convenience. Normally, the centre of gravity itself always locates well below the earth's surface. Its height (coordinates along orthogonal meridians) above (within) the equatorial plane is (are) given in the left (right) map.

Figure 8a compares the length of the gravity vectors, as the distance between the gravity centre and the earth's centre. It is a rough measure of the concentration of the underlying variable on the earth's surface. It also helps figuring out the radius of the inner-earth imaginary concentric sphere

[5]To avoid potential jumps in the final series, we smooth the transition from one database to the other by using a mix of both cell GDP data sets for overlapping decades 1990 and 2000. For the year 1990, we calculate final cell GDP as 70% of Maddison/HYDE cell GDP and 30% of G-Econ cell GDP, while for the year 2000 we calculate it as 30% Maddison/HYDE cell GDP and 70% G-Econ cell GDP.

[6]To avoid potential jumps in the final series, we smooth the transition from one database to the other by using a mix of both cell CO_2 data sets for the years 1970, 1980 and 1990, as we did for GDP. For 1970 (1980, 1990), we calculate final cell CO_2 emissions as 75% (50%, 25%) of CDIAC/HYDE cell emissions and 25% (50%, 75%) of EDGAR cell emissions.

TABLE 2 Summary statistics (cell level): Population (persons), GDP (1990 US$) and CO_2 (gigagrams), 1820–2010

Year	Variable	Obs.	Mean	*SD*	Min	Max
1820	Cell population	2,120,531	489.5	3,643.4	0	772,909
	Cell GDP	2,120,531	345,335.5	1.58E + 07	0	2.25E + 10
	Cell CO_2	2,120,531	0.007	0.37	0	118.9
2010	Cell population	2,120,531	3,409.6	59,676.9	0	5.84E + 07
	Cell GDP	2,120,531	3.06E + 07	1.35E + 09	0	1.11E + 12
	Cell CO_2	2,120,531	4.83	188.7	0	125,099

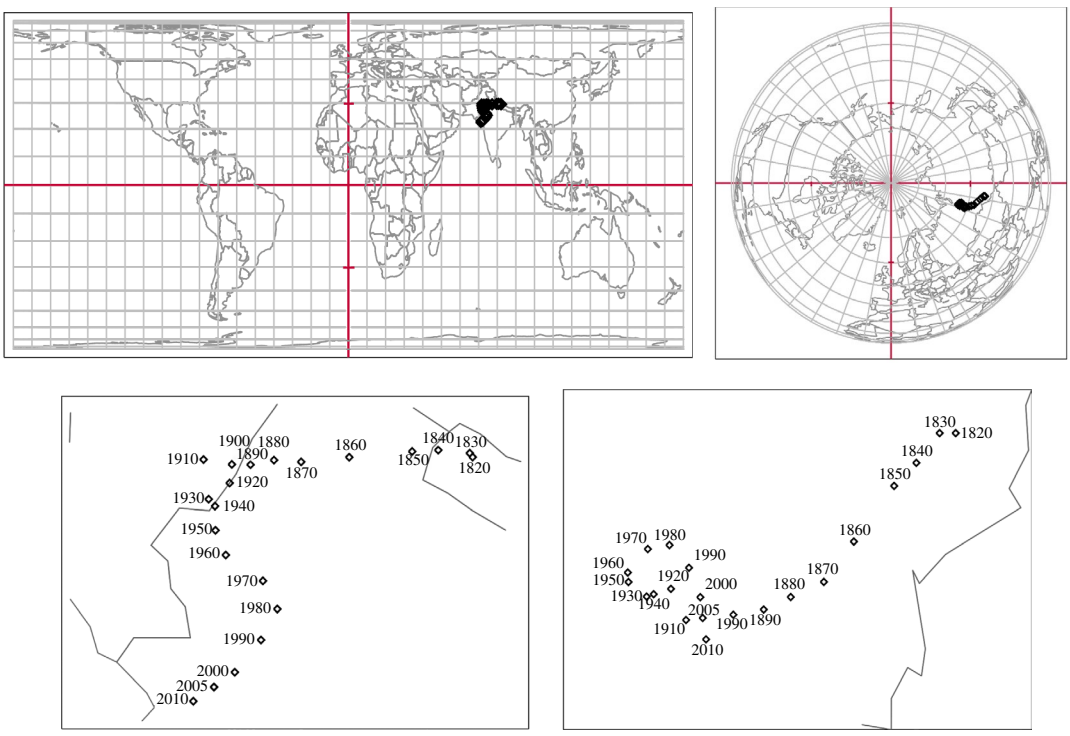

FIGURE 5 Centre of gravity for population [Colour figure can be viewed at wileyonlinelibrary.com]

upon which the centre of gravity locates. Figure 8b compares the speed of the gravity centres, that is the distance they cover per decade.

Regarding interpretation of trends, the coordinates of the world centre of gravity being a weighted average of individual cell's coordinates, it is intuitive that changes over time are mostly driven by variations in (large) country shares.[7] To condense presentation, we will only refer to the most important changes in the text below. The interested reader can also refer to the Appendix for the evolution of the share of the largest countries.

[7]In theory, within-country variation should also be addressed, but in practice, most of the variation comes from between-country changes. See also Grether et al. (2012) for a more in-depth discussion of the underlying drivers and a decomposition of changes in the economic centre of gravity into between-continent and within-continent effects.

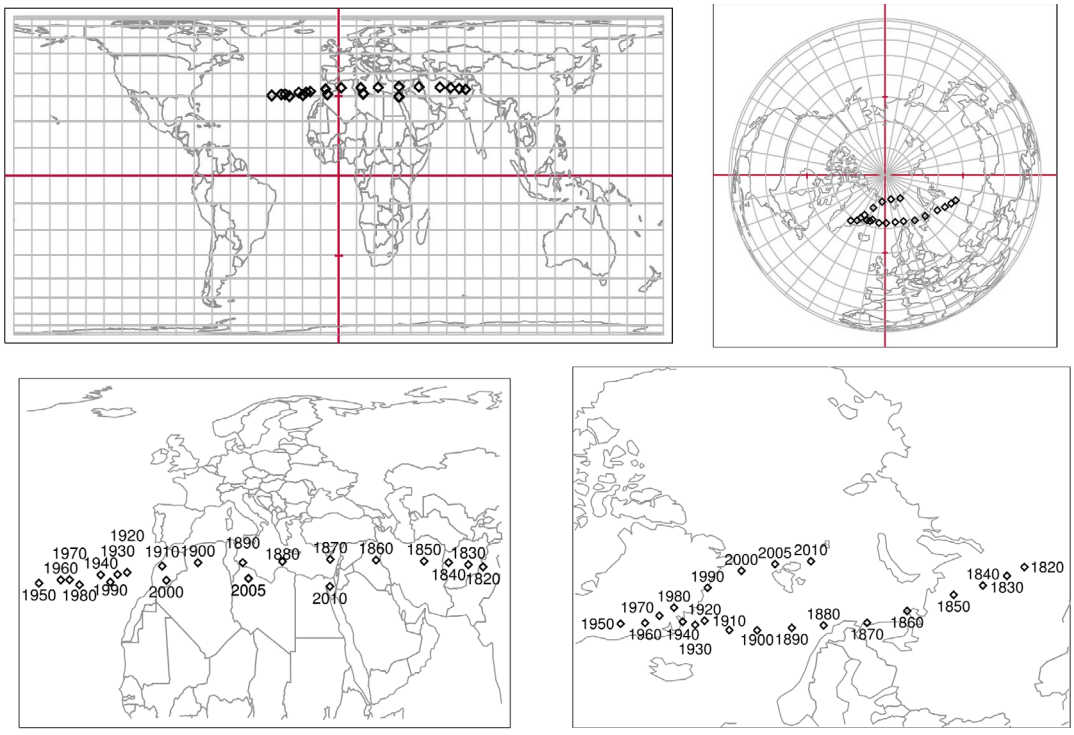

FIGURE 6 Centre of gravity for GDP [Colour figure can be viewed at wileyonlinelibrary.com]

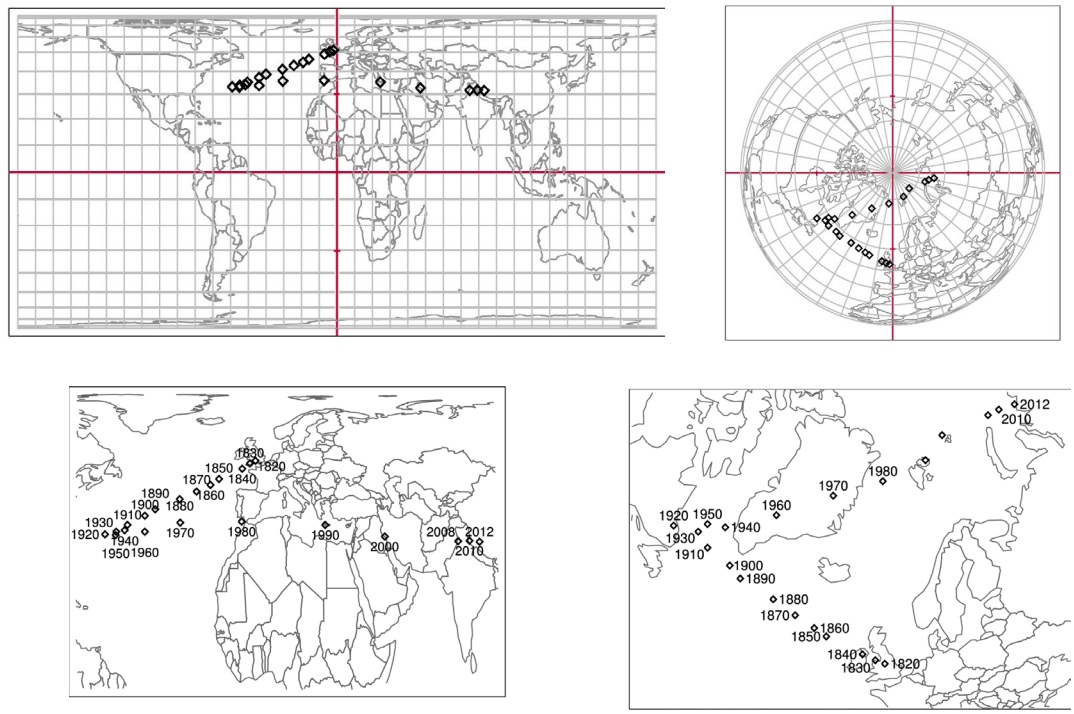

FIGURE 7 Centre of gravity for CO_2 emissions [Colour figure can be viewed at wileyonlinelibrary.com]

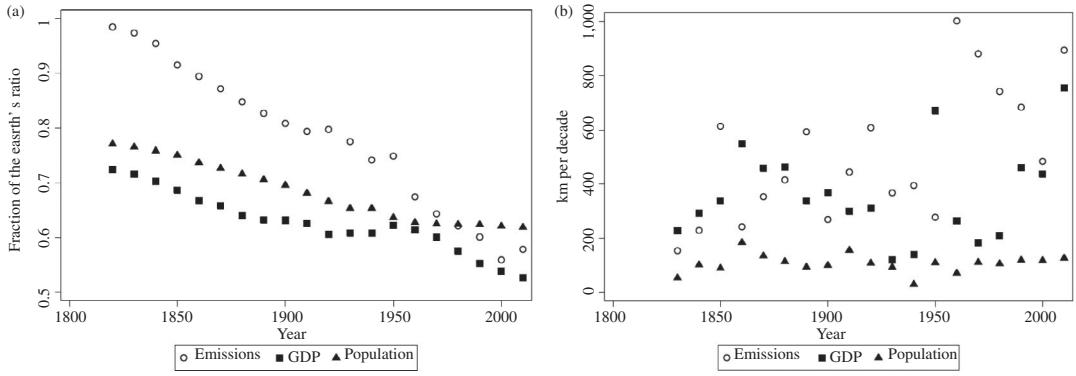

FIGURE 8 Length and speed for the centres of gravity. (a) Length. (b) Speed

4.1 | Population

As could be expected, the population centre of gravity is basically located under Asia (Northern India in the left maps and along the Russian–Kazak frontier in the right maps). At the beginning of the period, its length is close to 5,000 km, that is around 0.75*R*, where *R* is the earth's radius (6,371 km). This is the result of 0.5*R* elevation over the equatorial plane (corresponding to a Northern latitude of 30°) and approximately 0.6*R* rightward orientation on the projection of the 90° meridian (the coordinate along the projection of the Greenwich meridian is almost negligible). In short, human population is initially quite concentrated in the Asian part of the Northern Hemisphere.

The bottom maps reveal a small but steady shift during the sample period, in two distinct phases. During the first phase, which lasts until 1910, the centre of gravity shifts westward, with no latitudinal change. This is consistent with the gradual decline of China and India, whose combined share in world population drops from 55% to 40% along that subperiod. It is also concomitant with a leftward shift of the horizontal component of the left maps and a corresponding decline in the length of the gravity vector by around 15%. That is, human population becomes more homogeneously spread, with a decline in Eastern and a rise in Western locations, in particular the USA.

During the second phase, starting in 1920, there is a clear Southern shift, slightly eastward until 1980, and westward since then. This is consistent with Western countries plateauing in terms of population, the combined share of China and India remaining roughly constant, and a relative increase in Southern countries in East Asia first, and in Africa second. Overall, there is again an increase in the dispersion of human population, although the decline of the length of the gravity vector is more moderate than in the first phase.

These shifts in the demographic gravity centre are consistent with historical trends, but of modest magnitude, with an average speed of less than 200km per decade. The trends exhibited by the other two variables reveal more profound changes.

4.2 | Gross domestic product

The trajectory of the economic centre of gravity is also in two phases, but the striking features are that apparent distances covered are far larger than for the demographic centre, whereas the elevation upon the equatorial plane is almost unchanged, with most points locating along the 30°N parallel on left-hand side maps. Starting in 1820, the location is almost identical to the demographic centre of gravity, reflecting the small differences in GDP per capita across countries prior to the industrial

revolution. Then, the Big Divergence leads to a strong Western shift of the economic gravity centre, with a speed two to three times faster than for the demographic centre of gravity, and over a longer period. Although the process slows over the 1930s and 1940s, the immediate aftermath of World War II brings its last big Western push, with a 1950 location close to the middle of the Atlantic. During that same subperiod, the combined share of China and India in world GDP dropped from 45% to less than 10%, while that of the USA increased from a few percentage points to more than 25%.

Since 1950, the eastward shift has been steady, driven by European reconstruction first and then by the Asian comeback. It seems to accelerate a lot between 2000 and 2010, when the centre of gravity jumps by more than 40° of longitude. However, while interpreting left maps, one has to remember that longitudes are not a precise concept in terms of distances. It does not only depend on latitude (which is here roughly constant), but also on distance from the north–south axis, that is the inward location of the gravity centre within the sphere, which is indicated on the right map. And, between 2000 and 2010, it happens that the centre of gravity gets quite close to the earth centre, ending a continuous decrease in the length of the vector since 1950. As a result, the effective speed in 2010 remains less than in 1950; that is, it is indeed large but not extraordinarily so. This explains the apparent jump and illustrates again how relying on a unique map to represent a three-dimensional movement is misleading.

4.3 | CO_2 emissions

The trajectory of the centre of gravity for emissions is even more remarkable than for GDP. It is initially an almost purely British phenomenon, with a centre of gravity locating just underneath the UK, with a length corresponding to 98% of the earth's ratio. As the industrial revolution spreads, and use of coal as the main energy source, this centre begins its descent towards the south-west and the earth's centre. Its most westward location is in 1920, when its projection gets close to the US coast and its length has decreased to 81% of the earth's ratio. During that first period, the speed is similar to that recorded for the economic centre of gravity, although larger for the last two decades of the subperiod (1910 and 1920). Overall, the nineteenth century is a period during which GDP and CO_2 emissions tend to evolve synchronously and westward. This is due to the progressive replacement of the UK by the United States as the major source of world emissions. US dominance peaks in 1920, with a share of 50% of world emissions.

Comparative dynamics of GDP and emissions are altered after World War I. While economic expansion continues its westward trend, the centre of gravity of CO_2 emissions shifts towards the east in 1930 and 1940. This suggests a decoupling between economic activity and pollution, which is probably linked with the early adoption of oil as an alternative, less emission-intensive, source of energy by the United States (i.e. the major polluter), while other major polluters remain more coal-dependent. Indeed, according to Smil (2010), the share of coal in US energy supply peaks in 1910, while it does so only 40 years later in the UK and the USSR. As a result, the share of the United States in world emissions declines strongly in 1930–40, whereas its GDP share remains stable. This explains the earlier reversal of the emission centre of gravity with respect to the economic one. Economic trends remain powerful however, and the US growth spurt following the end of World War II temporarily interrupts the eastern trend in 1950, when both centres of gravity shift westward again, albeit more modestly for the emission centre.

From 1950 onward, the emission centre of gravity is heading east, as is the economic one. This is in line with a decline in US dominance in terms of both GDP and emissions, although the decline is a lot larger for emissions, with a US share in world emissions dropping from above 40% in 1950 to 20% in 1980. This coincides with very large distances covered by the emission centre of gravity, close to

1,000 km per decade, as reported by Figure 8. This suggests again that the transition towards non-coal energy sources such as oil and gas has been quicker in the United States compared to other large emitters (the share of coal falls below 50% as early as 1940 for the United States, but only in 1960 for the UK or Japan, and 1970 for Russia, see Smil, 2010).

During the first two decades following the end of the Cold War, 1990 and 2000, the eastern shift is slowed down, as the US share in world totals either stabilises for emissions or even increases slightly for GDP. This is in line with a pause in the erosion of US dominance and the demise of the USSR.[8] But the movement accelerates again in the last decade, 2010, for both GDP and emissions. This corresponds to the rise of Asian countries, in particular China, which remains heavily dependent on coal as an energy source. By the end of the sample period, the emission centre of gravity locates quite close to the demographic centre of gravity.

In a nutshell, the evolution of the emission centre of gravity suggests radical changes in the spatial distribution of CO_2 emissions on the earth's surface. In two centuries, it shifts from an extremely concentrated location to one which is strikingly similar to the distribution of world population.

5 | SPATIAL IMBALANCES: MEASUREMENT AND DISCUSSION

People are unequally spread across the planet's surface. This encapsulates into a location of the demographic centre of gravity which is roughly stable over time, at $0.5R$ ($R = 6{,}371$ km) above the equatorial plane and $0.5R$ to the right of the Greenwich meridian. If GDP and emissions were equally shared among people, the corresponding centres of gravity would locate at the same place, that is below Northern India, at roughly 70% from the centre of the earth. This is not what has happened during the last two centuries. From there the idea of using distance between the demographic centre of gravity and the comparison one as a proxy for spatial imbalances characterising the per capita distribution of the underlying variable (either GDP or emissions).

More specifically, following Zhao et al. (2003), we define the index of spatial imbalances as the ratio between the actual distance between the demographic centre of gravity and the one it is compared to, and the potential maximum for that distance, that is the length of the demographic centre of gravity vector plus the earth's radius.[9] Applied to GDP and emissions, this leads to the values reported in Figure 9.

What happens for GDP confirms the trend reversal pattern already identified in Figure 6. Spatial imbalances start below 10% and then increase during the Great Divergence, as economic growth takes off in Western countries and their offshoots. The peak is reached in 1950, with an index slightly over 50%. After that, European and then most importantly Asian catch-up decreases spatial imbalances back to 20% at the end of the period.

The temporal pattern for emissions is distinct in that it starts from a large level of close to 50% in 1820. The rest of the trajectory is qualitatively similar to GDP, that is also an inverted-u shape, but with three differences. First, the rising phase is less steep, with a peak at 60%. This is due to the fact that, apart from

[8]We warn again the reader against using the left map only to estimate distances covered by the emission centre of gravity in 1990 and 2000. They appear large, in particular in contrast with 1960. However, as shown by the right map, it is a typical 'wiper' effect due to the fact that the centre of gravity locates closer and closer to the earth's centre from 1950 onward. In reality, distances covered are considerably smaller in 1990 or 2000 than in 1960 (see Figure 8).

[9]For example, if the demographic centre of gravity is denoted by D, the economic centre of gravity is denoted by G, and the earth's centre is denoted by O, then the index of spatial imbalances for GDP is given by $\left\|\overrightarrow{DG}\right\| \Big/ \left[\left\|\overrightarrow{DO}\right\| + R\right]$, where R is the earth's radius.

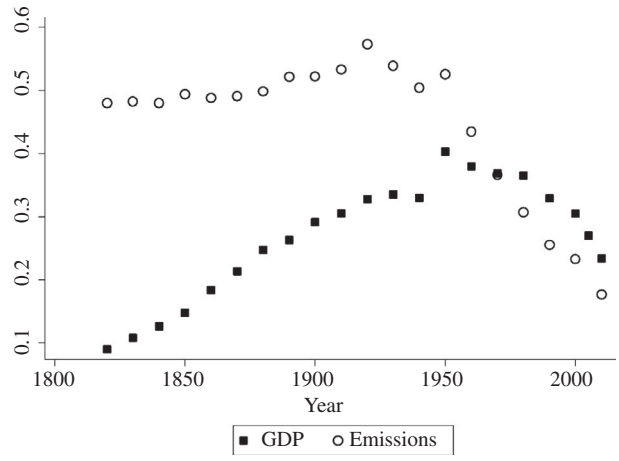

FIGURE 9 Indices of spatial imbalances

going west, which increases the index, the centre of gravity is also going southward, which decreases the index. Second, as already noticed in Figure 7, the peak is reached in 1920, not 1950. Third, the decreasing phase is steeper, with a final index of spatial imbalances for emissions around 10% in 2010.

Intuitively, if data had been available for earlier centuries, it is probable that the pattern of spatial imbalances for emissions would have looked even more similar to that for GDP. After all, before any country started its industrial revolution, differences in emissions per capita across countries were probably not large, implying a low level of spatial imbalances. This suggests a kind of leading role of emissions with respect to GDP over a long time span.

Although no formal analysis has been performed, the interpretation would be as follows. Start from a preindustrial world where production and emissions are roughly homogeneous across people. Then, technological innovation and the use of fossil fuels give an early boost to Western countries. The impact on emissions is immediate, while the effect on production takes several decades to materialise. During the rest of the nineteenth and early twentieth centuries, as the west industrialises alone, emissions and production go hand in hand. Then, rapid adoption of less emission-intensive energy sources (oil and gas rather than coal) by the United States sends back the emission centre of gravity towards the east as early as the 1930s. Economic activity is characterised by more inertia, but when it starts to shift back as well after 1950, this accelerates further the eastern movement in emissions, also enhanced by the shift of more emission-intensive manufacturing activities towards Asia. As it happens, after a long period of divergence, both the economic and the emission centres of gravity seem to be dragged back to their initial 1820 location determined by demography.[10]

The above trends are confirmed when using alternative conventions regarding the smoothing shift from CDIAC to EDGAR data for emissions, or from Maddison to G-Econ data for GDP. Note that temporal patterns for the demographic and economic centres of gravity are similar to those identified by Grether et al. (2012), even though the latter did not rely on the Hyde database to capture within-country changes in spatial distributions. Moreover, as recently illustrated by Sauter, Grether, and Mathys (2016), alternative hypothesis regarding the spatial distribution of emissions hardly affects overall patterns. Therefore, given data limitations, our results can be considered as reasonably robust.

[10]The extreme spatial concentration of emissions at the beginning of the sample period is due to the narrow definition of CDIAC historical data, limited to fossil fuel consumption and cement production only. However, to our knowledge, it is the best historical data on CO_2 emissions available at present.

6 | CONCLUSIONS

Taking the best of the available databases, this paper proposes for the first time distortion-free representations of the trajectories of the world demographic, economic and emission centres of gravity over the last two centuries. Technological innovation, energy transition, structural change and wars are the main factors underlying observed trends and turning points. In a nutshell, it is as if demography acts like a long run anchor, while emissions and GDP are two outcome variables of a technological diffusion process which increases spatial inequalities during the nineteenth century and progressively decreases them during the twentieth century. The patterns revealed allowing for a quantification of the structural shifts underpinning the Great Divergence, but with a different time-frame depending on the underlying variable. When emissions are used, they suggest a deeper divergence, which starts well before 1820 and leads to an Eastern reversal as early as 1920. These results are in line with current research on the geopolitical origins of capitalism (e.g. Anievas & Nisancioglu, 2015). Based on these results, we suggest the following lines of further research.

Trade and FDI activities should be taken into account. For historical reasons first, as they were crucial in promoting the technological innovations at the root of the Industrial Revolution and the Great Divergence (e.g. O'Rourke, Rahman, & Taylor, 2012). For contemporaneous relevance also, as they are key elements of the globalisation process, with a global diffusion of the value chain that has made necessary the computation of trade in value-added flows (see OECD & WTO, 2013). Refining centres of gravity calculations in light of these increased interdependences may unveil interesting trends, for example to trace the potential consequences of the 'belt and road' policy recently adopted by China (The Economist, 2017), or to capture consumption-based rather than production-based CO_2 emission estimates (e.g. Wiebe & Yamano, 2016), a distinction that is at the heart of climate change negotiations today.

Moreover, further research should aim at including even more variables, to capture the many dimensions of human activities and interdependences. To mention just one, in a world that has become more multipolar, large nations rely increasingly on geopolitical power (energy, geography, nuclear and military force) or soft power instruments (trade again, but also diplomacy, advertising, or cultural promotion) to improve their relative positions (e.g. Reynaud & Vauday, 2009 or Wang, Cao, & Ge, 2015). This may lead to a frequent rebalancing of socioeconomic influences at the worldwide level. By synthesising the spatial distribution of any variable into a single point, the world centre of gravity approach allows to reveal interesting dynamics within this changing context.

ACKNOWLEDGEMENTS

We thank Jim de Melo, Gabriel Felbermayr, Milad Zarin and the editor David Greenaway for insightful comments, as well as the Swiss National Science Foundation for financial support under grant 100018-136625. The usual caveats apply.

DATA AVAILABILITY STATEMENT

All raw data used in the present paper can be accessed through the URLs provided in the references.

ORCID


Jean-Marie Grether https://orcid.org/0000-0002-2601-3585

REFERENCES

Anievas, A., & Nisancioglu, K. (2015). *How the west came to rule—the geopolitical origins of capitalism*. Chicago, IL: University of Chicago Press.

Baier, S. L., & Bergstrand, J. H. (2009). Bonus vetus ols: A simple method for approximating international trade-cost effects using the gravity equation. *Journal of International Economics*, *77*(1), 77–85. https://doi.org/10.1016/j.jinteco.2008.10.004

Barrett, S., & Stavins, R. (2003). Increasing participation and compliance in international climate change agreements. *International Environmental Agreements: Politics, Law and Economics*, *3*(4), 349–376. https://doi.org/10.1023/B:INEA.0000005767.67689.28

Boden, T., Marland, G., & Andres, R. (2013). *Global, regional and national fossil-fuel CO_2 emissions*. Tech. rep., Carbon Dioxide Information Analysis Center, Oak Ridge National Laboratory, U.S. Department of Energy, Oak Ridge, TN. Retrieved from CDIAC website: https://cdiac.ess-dive.lbl.gov/trends/emis/overview_2010.html

Bradshaw, M. (2014). *Global energy dilemmas: Energy security, globalization, and climate change*. Cambridge, UK: Polity.

Broadberry, S. (2013). *Accounting for the great divergence* (Economic history working paper no 184–2013). London School of Economics. http://eprints.lse.ac.uk/54573/1/WP184.pdf

Ellis, E. C., Kaplan, J. O., Fuller, D. Q., Vavrus, S., Goldewijk, K. K., & Verburg, P. H. (2013). Used planet: A global history. *Proceedings of the National Academy of Sciences of the USA*, *110*(20), 7978–7985. https://doi.org/10.1073/pnas.1217241110

European Commission, Joint Research Centre (JRC)/Netherlands Environmental Assessment Agency (PBL) (2011). *Emission database for global atmospheric research (EDGAR), release version 4.2*. Retrieved from http://edgar.jrc.ec.europa.eu

GADM (2012). *GADM database of global administrative areas, version 2.0*. Retrieved from www.gadm.org

G-Econ (2011). *Geographically based economic data*. Retrieved from http://gecon.yale.edu

Grether, J.-M., & Mathys, N. A. (2010). Is the world's economic centre of gravity already in Asia? *Area*, *42*(1), 47–50. https://doi.org/10.1111/j.1475-4762.2009.00895.x

Grether, J.-M., & Mathys, N. A. (2011). On the track of the world's economic center of gravity. In O. de La Grandville (Ed.), *Frontiers of economics and globalization*, Vol. *11*, (pp. 261–287). *Economic growth and development.* London, UK: Emerald Group.

Grether, J.-M., Mathys, N. A., & Lutzelschwab, C. (2012). L'essor et le déclin de l'occident: une perspective géographique. *Revue D'économie Du Développement*, *2*, 31–56.

Klein Goldewijk, K., Beusen, A., van Drecht, G., & de Vos, M. (2011). The Hyde 3.1 spatially explicit database of human-induced global land-use change over the past 12,000 years. *Global Ecology and Biogeography*, *20*(1), 73–86.

Lindmark, M. (2004). Patterns of historical CO_2 intensity transitions among high and low-income countries. *Explorations in Economic History*, *41*(4), 426–447. https://doi.org/10.1016/j.eeh.2004.01.003

Maddison, A. (2010). *Statistics on world population, GDP and per capita GDP*. Retrieved from http://ggdc.net/MADDISON/

Matthews, H. D., Graham, T. L., Keverian, S., Lamontagne, C., Seto, D., & Smith, T. J. (2014). National contributions to observed global warming. *Environmental Research Letters*, *9*(1), 1–9. https://doi.org/10.1088/1748-9326/9/1/014010

Mattoo, A., & Subramanian, A. (2012). Equity in climate change: An analytical review. *World Development*, *40*(6), 1083–1097. https://doi.org/10.1016/j.worlddev.2011.11.007

Nordhaus, W., Azam, Q., Corderi, D., Hood, K., Makarova, N., Mohammed, M., …Weiss, J. (2006). *The G-Econ database on gridded output: Methods and data*. Retrieved from http://gecon.yale.edu

OECD & WTO (2013). *Measuring trade in value added: An OECD-WTO joint initiative*. Retrieved from http://www.oecd.org/sti/ind/measuringtradeinvalue-addedanoecd-wtojointinitiative.htm

O'Rourke, K. H., Rahman, A. S., & Taylor, A. M. (2012). *Trade, technology and the great divergence*. (Departmental Working Papers 35). United States Naval Academy Department of Economics. Retrieved from https://ideas.repec.org/p/usn/usnawp/35.html

Quah, D. (2011). The global economy's shifting center of gravity. *Global Policy*, *2*(1), 3–9.

Reynaud, J., & Vauday, J. (2009). Geopolitics and international organizations: An empirical study on IMF facilities. *Journal of Development Economics*, *89*(1), 139–162. https://doi.org/10.1016/j.jdeveco.2008.07.005

Sauter, C., Grether, J.-M., & Mathys, N. A. (2016). Geographical spread of global emissions: Within- country inequalities are large and increasing. *Energy Policy*, *89*(C), 138–149. https://doi.org/10.1016/j.enpol.2015.11.024

Smil, V. (2010). *Energy transition: History, requirements, prospects*. Santa Barbara, CA: Praeger.

Snyder, J. (1987). *Map projections: A working manual. No. 1395 in US Geological Survey Professional Paper*. US Government Printing Office, Washington, DC. Retrieved from https://pubs.usgs.gov/pp/1395/report.pdf

Studer, R. (2015). *The great divergence reconsidered: Europe, India, and the rise to global economic power*. Cambridge, UK: Cambridge University Press.

The Economist (2017). *The new silk route: All aboard the belt-and-road express*. 4 May. Retrieved from https://www.economist.com/china/2017/05/04/china-faces-resistance-to-a-cherished-theme-ofits-foreign-policy

The Maddison Project (2013). *2013 version*. Retrieved from http://www.ggdc.net/maddison/maddison-project/home.htm

Wang, S., Cao, Y., & Ge, Y. (2015). Spatio-temporal changes and their reasons to the geopolitical influence of China and the US in South Asia. *Sustainability*, *7*(1), 1064–1080. https://doi.org/10.3390/su7011064

Wiebe, K. S. & Yamano, N. (2016). *Estimating CO_2 emissions embodied in final demand and trade using the OECD ICIO 2015: Methodology and results* (OECD Science, Technology and Industry Working Paper No. 2016/5). Retrieved from OECD website: https://www.oecd-ilibrary.org/docserver/5jlrcm216xkl-en.pdf?expires=1566977487&xml:id=id&accname=guest&checksum=9B6AA1B681902233E9CCCD58F705C40A

Zhao, Z., Stough, R. R., & Li, N. (2003). Note on the measurement of spatial imbalance. *Geographical Analysis*, *35*(2), 170–176.

How to cite this article: Sauter C, Grether J-M, Mathys NA. A global compass for the great divergence: Emissions versus production centres of gravity 1820–2008. *World Econ*. 2019;42:2818–2834. https://doi.org/10.1111/twec.12860

APPENDIX

Figure A1 reports, for each variable of interest, the evolution of the share of the largest six countries in world totals over the sample period.

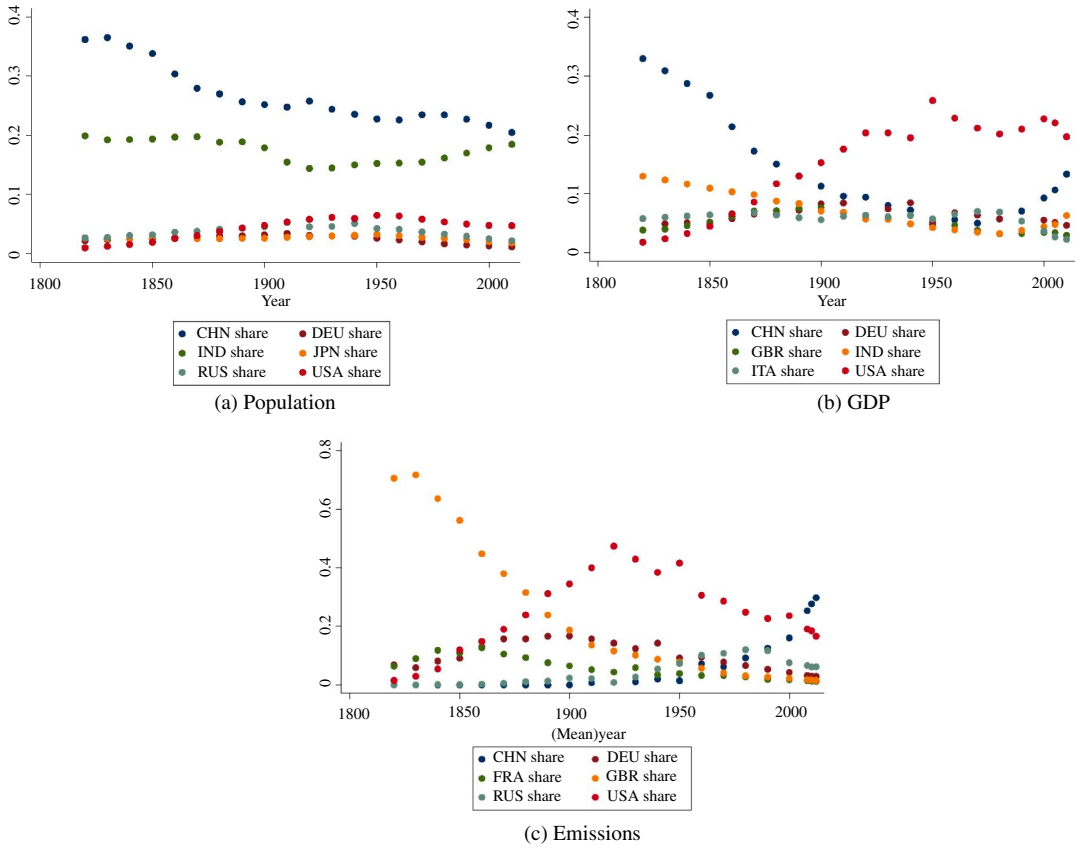

FIGURE A1 Shares of major countries in world totals 1820–2010 [Colour figure can be viewed at wileyonlinelibrary.com]